Arabian Journal of Chemistry (2021) **14**, 103109

King Saud University

Arabian Journal of Chemistry

www.ksu.edu.sa
www.sciencedirect.com

ORIGINAL ARTICLE

Novel stand-alone PVA mixed matrix membranes conjugated with graphene oxide for highly improved reverse osmosis performance

Wail Falath [a,b]

[a] *Center of Research Excellence in Desalination and Water Treatment, King Fahd University of Petroleum and Minerals (KFUPM), Dhahran 31261, Saudi Arabia*
[b] *Department of Mechanical Engineering, King Fahd University of Petroleum & Minerals, Dhahran 31261, Saudi Arabia*

Received 15 December 2020; accepted 24 February 2021
Available online 4 March 2021

KEYWORDS

Poly (vinyl alcohol) (PVA);
Graphene oxide;
RO membranes;
Biofouling;
Chlorine resistance;
Pluronic F-127

Abstract In this research, an innovative Poly (vinyl alcohol) (PVA) reverse osmosis (RO) membrane with exceptional attributes was fabricated. Graphene Oxide (GO) nanosheets and Pluronic F-127 were infused within crosslinked PVA to fabricate thin film mixed matrix membranes. The newly synthesized membranes were evaluated in terms of several parameters like surface roughness, hydrophilicity, salt rejection, water permeability, Chlorine tolerance and anti-biofouling property, utilizing a dead-end RO filtration unit. Typical characterization techniques were used to assess the characteristics of the membranes. These include SEM, AFM, contact angle measurements and mechanical strength analysis. The conjugation of Pluronic F-127 and GO enhanced the overall performance of the membranes. The modified membranes surfaces had less roughness and higher hydrophilicity in comparison with the unmodified ones. This research showed that membranes that contained 0.08 wt% and 0.1 wt% GO exhibited superior selectivity, mechanical strength, Chlorine tolerance and anti-biofouling property. The truly significant outcome to evolve from this investigation is that improvements have been accomplished while PVA was used as a stand-alone RO layer without the use of any substrate. This study showed that crosslinking of PVA and modifying it with proper fillers overcame the common PVA downsides, primarily swelling and rupture under exceptionally high pressure.

1. Introduction

World-wide water scarcity is increasingly becoming the most critical problem affecting people around the world. Coupling this with the exponential growth in population and economy yields a recipe for calamitous fresh-water dearth. Global demand of fresh water is anticipated to jump from 4.5 trillion

E-mail address: wfallata@kfupm.edu.sa
Peer review under responsibility of King Saud University.

Production and hosting by Elsevier

https://doi.org/10.1016/j.arabjc.2021.103109

m^3 to 6.9 trillion m^3 by 2030 (Shannon, 2008; Misdan et al., 2012).

Only 2.5% of earth's surface, is fresh-water and it is not easily accessible. The reason is the fact that most of the fresh water is accumulated as glaciers or is very deep underground (Shannon, 2008; Oki and Kanae, 2006; Subramani and Jacangelo, 2015). With this substantial increase in fresh-water demand, an effort to develop desalination technologies is necessary.

Reverse Osmosis (RO) is the predominant technology for desalination nowadays. It is becoming the major desalination technology over conventional thermal technologies. Due to desalination process developments and major cost and energy reductions, RO processes attract interests commercially (Lee et al., 2011; Malaeb and Ayoub, 2011; Kochkodan and Hilal, 2015; Matin, 2011). However, membrane fouling causes a cutback in performance of reverse osmosis (RO) membranes, which is a major concern. Due to fouling, the membranes need to be chemically cleaned and treated frequently. This eventually abridges the membrane's life, which increases the cost of the overall reverse osmosis process (Herzberg and Elimelech, 2007; Baker and Dudley, 1998). Most of the foulants, other than bio-foulants, can be removed or their effect can be minimized to some extent by pretreatment. Biofouling, on the other hand, is different. It is defined as the formation of bacteriological films onto membrane's surface or inside its pores. Microorganisms can withstand extreme conditions like temperatures ranging from −12 °C to 110 °C and pH ranging from 0.5 to 13. The attached microorganisms embed, and form biofilms. This means that the initially absorbed species are restrained and transformed from the solution into a semi-solid form (Baker and Dudley, 1998; Flemming, 2002; De Beer and Stoodley, 2006; Sadr Ghayeni, 1998). Biofilm formation causes several undesirable consequences on the RO process, such as flux decline, operating pressure increase, membrane biodegradation and loss of salt rejection (Ridgway, 1990). In this study, novel stand-alone PVA mixed matrix membranes infused with Pluronic F-127 and Graphene Oxide were fabricated by dissolution casting.

PVA has been utilized extensively in applications related to water purification, since it possesses superb properties, such as water-solubility, biodegradability, intrinsic hydrophilicity, good film-forming properties, good Chlorine tolerance, excellent fouling resistance and exceptional thermal, mechanical and chemical stability (Liu, 2014, 2013; Bolto, 2009; You, 2012; Bezuidenhout, 1998; Hu, 2012; Yee, 2014). Due to its very high hydrophilicity, swelling of PVA membranes is expected and it leads to an open structure that is not favorable, as the membrane loses its separation effectiveness. To solve such a problem, crosslinking of PVA is performed to generate a membrane that has the balance between permeability and selectivity (Cha et al., 1993; Gebben, 1985; Macho, 1994; Huang and Rhim, 1993; Korsmeyer and Peppas, 1981; Giménez et al., 1996).

Poloxamers or Pluronics are triblock amphiphilic copolymers comprising two polyethylene oxide blocks inclosing a polypropylene oxide block (PEO–PPO–PEO) as a monomer. Thus, the copolymer contains hydrophilic PEO parts and hydrophobic PPO parts. Unlike other Poloxamers and Pluronics, Pluronic F-127 (M_W 12,600) has a great hydrophilic/lipophilic balance value of 22, and superb extractability towards aqueous phase (Kim et al., 2006; Lv, 2007). Many researchers reported that the inclusion of Pluronic F-127 within PVA matrix improves the permeability and selectivity of the membranes. It is also used as a pore-forming agent (Lv, 2007; Iwasaki et al., 2003; Amanda, 2000; Ishihara et al., 1995; Yajima, 2002).

Graphene Oxide (GO) consists of nanosheets that attracted research interest in the area of water treatment membranes fabrication (Huang, 2019; Hegab and Zou, 2015; Li et al., 2016; Cohen-Tanugi and Grossman, 2015; Mahmoud, 2015). This is mainly due to its distinct inherent properties, such as superb surface area, good mechanical strength, abundant hydrophilic functional groups, and its capability to mitigate the progression of bacteria when it contacts the cells directly (Li et al., 2016). Coating membrane surfaces with GO improved Chlorine resistance and fouling resistance of the surfaces (Choi, 2013). In recent years, researchers investigated the incorporation of GO nano-sheets into polymer matrix to form separation membranes (Huang, 2019; Hu and Mi, 2013; Kim, 2013). Current research shows that GO inclusion enhances mechanical strength of matrices in many applications including bio-applications. Furthermore, It has been shown that GO-based nanomaterials were used to improve desalination processes due to their excellent mechanical stability ultrafast diffusion and other superb properties (Yang, 2021; Johnson and Hilal, 2021; Le, 2021; Presumido, 2020).

PVA has been used by many investigators as a surface modifier to improve surface hydrophilicity or as a coating on various membrane surfaces for numerous separation applications (Kang, 2012; Rajaeian, 2015; Liu, 2015; Li, 2014, 2010; Bano, 2014; Flynn, 2013; Pourjafar et al., 2012; Barona et al., 2012; Zhang, 2008; Shang and Peng, 2008, 2007; Guo, 2007; Anis et al., 2014). To the best of the author's knowledge, no investigation has been conducted on the utilization of PVA conjugated with Graphene Oxide as a stand-alone RO active layer for seawater desalination without using any ceramic or polymeric substrates. Crosslinked PVA has been conjugated with Graphene Oxide to mitigate common PVA limitations, mainly swelling and rupture under high pressure.

In this investigation, a unique PVA membrane conjugated with Graphene Oxide and Pluronic F-127 was fabricated for utilization in reverse osmosis conditions. The newly fabricated membranes were then characterized and analyzed using several techniques including contact angle measurements, X-ray diffractometry (XRD), atomic force microscopy (AFM), scanning electron microscopy (SEM) and mechanical testing. A dead-end RO permeation unit was used to assess the performance of the membranes, comprising permeation flux testing, selectivity and Chlorine and biofouling resistance measurements.

2. Experimental setup

2.1. Materials and reagents

Analytical grade Poly (vinyl alcohol) (Mw = 89000), Pluronic F-127 (average molecular weight: 12.6 kDa), bisphenol A diglycidyl ether (DGEBA) (crosslinker), sodium hypochlorite (NaClO) and dimethyl sulphoxide (DMSO) were attained from Sigma Aldrich (USA). Graphene Oxide (GO) sheets were obtained from Graphene Supermarket (Calverton, NY, USA), with flakes ranging in size from 0.3 to 0.7 μm and a ratio of

carbon to oxygen of 4:1. All chemicals were utilized as received.

2.2. Membrane fabrication

2.2.1. PVA crosslinking and infusion of Pluronic F-127

DGEBA (crosslinker) was incorporated into PVA solutions following the procedure detailed in a previous research conducted by the author and his collaborators (Falath et al., 2016, 2017). It has been shown that the optimum weight percentage of the crosslinker is 0.16 wt%. The optimization was performed to investigate the weight percent that yields best combination between permeability and selectivity. Pluronic F-127 was incorporated into the solution in a similar way and it was found that the optimal weight percentage was 6 wt% (Falath et al., 2016, 2017). Fig. 1 is a schematic diagram that shows the chemical reaction.

2.2.2. Graphene oxide conjugation with crosslinked PVA membrane

Table 1 shows various weight percentages of Graphene Oxide that were infused to the previously prepared solution that contains crosslinked PVA and Pluronic F-127 (6 wt%) to fabricate the mixed matrix membranes. Graphene Oxide was infused into the solution at 60 °C with continuous stirring for 5 h until it was dissolved completely and a homogeneous solution was formed. The membrane casting followed the dissolution casting methodology the author and his collaborators used in their previous work (Falath et al., 2016, 2017).

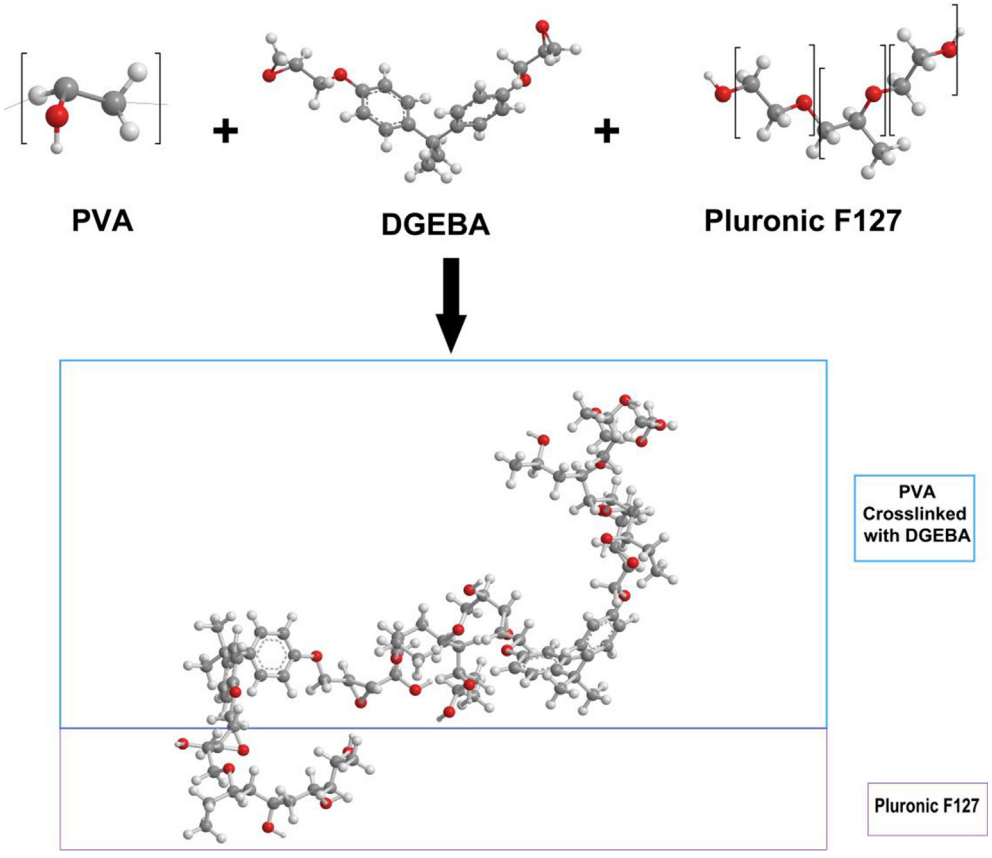

Fig. 1 Schematic diagram of PVA crosslinking and the intermolecular hydrogen bonding with Pluronic F-127.

Table 1 Graphene Oxide wt% in PVA solution and labeling.

	Weight percentages (wt%)				
Graphene Oxide*	0.02	0.04	0.06	0.08	0.10
Labels	PVA-G1	PVA-G2	PVA-G3	PVA-G4	PVA-G5

*with 6 wt% Pluronic F-127 and 0.16 wt% DGEBA.

2.3. Membranes characterization

2.3.1. Contact angle measurements

To test the hydrophilicity of membrane surfaces, A Goniometer (Digidrop, KSV Instruments) that calculates sessile drop contact angles of the membrane surfaces has been utilized. To calculate the contact angle, the average of right and left angles of the drop were taken into consideration for the fitting done by the software. Three readings for each sample were rounded to report contact angle in degrees. All readings were taken immediately after the droplet contacts the surface of the membrane to ensure accuracy.

2.3.2. X-ray diffraction measurements

The synthesized mixed matrix membranes structure was characterized using X'pert PRO Diffractometer (PANalytical). A monochromatized CuK α1 radiation was utilized with 1.540 Å wavelength. The voltage and current were 40 kV and 40 mA, respectively. The range of scanning was from 4° to 80°.

2.3.3. Scanning electron microscope (SEM)

SEM images of the membranes were attained utilizing (S-3400N Hitachi, USA) SEM. The SEM functions under low vacuum mode to characterize the samples. Before placing the samples inside the SEM, gold sputtering was done for 120 s to be sure that no surface charging takes place.

2.3.4. Atomic force microscopy (AFM)

AFM analysis was conducted using (Digital Instruments, US) AFM with standard tapping mode to characterize the roughness of the surfaces. At each down stroke of each sinusoidal cycle at 350 kHz resonant frequency, a cantilever momentarily touches the surface. The resolution of the scanned images was 512 × 512 pixel. Root-mean-square surface roughness (R_q) is obtained by the following equation (Fang and Chang, 2003):

$$R_q or RMS = \sqrt{\frac{1}{n}\sum_{i=1}^{n} z_i{}^2}$$

Here z_i is the extent of the i^{th} lowest or greatest deviation, while n denotes the discrete variations number.

2.3.5. Mechanical testing

Mechanical stability was characterized using a Tensile testing equipment (Instron 5567) that was equipped with a load cell that has a capacity of 10 kN. The stiffness of the membranes denoted by the Young's modulus was calculated by the software. ASTM D-638 standard was utilized in tensile testing. The gauge length of the sample was 50 mm while the width was 10 mm. Three samples were cut from each fabricated membrane. The crosshead speed was 10 mm/min. Membrane's thickness was kept at 0.1 mm for all samples. Tensile testing was performed at ambient temperature. Stiffness was calculated in triplicates from tensile curves.

2.3.6. Permeability and selectivity testing

To assess the RO performance of the newly fabricated membranes, a dead-end RO filtration (HP4750, Sterlitech, WA, US), as shown in Fig. 2, was utilized to assess the permeability and selectivity of the newly fabricated membranes. The filtration unit is made from stainless steel 316. Membrane's active surface area was 14.6 cm^2. Commercially available natural sea salt (3.28 wt%) was utilized to simulate seawater and the pressure was kept at 800 psi. The salinity of the feed solution and the applied pressure were chosen to imitate the average seawater salinity and the typical applied pressure at RO plants, respectively. Permeate flux of the membrane was calculated by the subsequent relation:

$$F\left(\frac{L}{m^2 h}\right) = \frac{V(L)}{A(m^2) x t(h)}$$

where F is the permeate flux across the membrane per unit area (A) per unit time (t). Commonly, the abbreviation (LMH) is used to represent the unit of water flux. Selectivity was assessed by gauging permeate's salinity and comparing it to the salinity of the feed. Salinity testing was conducted by a salinity meter. Each reported result was the average from at least three samples after 8 h of operation to make sure steady state is achieved.

2.3.7. Biofouling resistance testing

Biofouling resistance activity was assessed by measuring optical density (OD) by a spectrophotometer, while using Escherichia coli (E. coli) as a model bacterium. Testing procedure followed JIS L 1902:2002 methodology and is detailed elsewhere (Falath et al., 2016, 2017).

2.3.8. Chlorine resistance test

The exposure to high concentrations of Chlorine for a short duration is equivalent to the exposure to low concentrations of Chlorine for a longer duration, as has been reported by many researchers (Petersen, 1993; Liu, 2011). Therefore, for lab testing purposes, it is more convenient to test membranes at high concentrations of Chlorine for a short time to assess Chlorine tolerance of membrane surfaces. To prepare the Chlorinated solution, commercial NaClO solution was diluted by mixing with distilled water. HCl (0.1 M) was used to adjust the pH of the prepared hypochlorite solution to become 4.0 to assure more harsh environment (Augustine, 2012). To assess Chlorine resistance, the selectivity of the membranes was assessed before and after Chlorination. If the selectivity percentage is almost maintained after Chlorination, it indicates that the surface of the membrane was not negatively affected by the exposure to Chlorine. Before Chlorine Exposure, membranes selectivity was assessed using 2000 mg/L NaCl solution. After rinsing the membranes, Chlorination takes place at 2000 mg/L hypochlorite solution for 2 h while keeping the pH at 4.0 at ambient temperature. Afterwards, the selectivity was assessed once more with 2000 mg/L NaCl solution.

3. Results and discussion

3.1. Contact angle analysis

Contact angle determination is a tool that is used to compute and assess the wettability and the hydrophilicity/hydrophobicity of a solid surface (Kwok and Neumann, 1999). Commercially available RO membranes are mostly hydrophobic which makes them susceptible to adsorption by biofoulants.

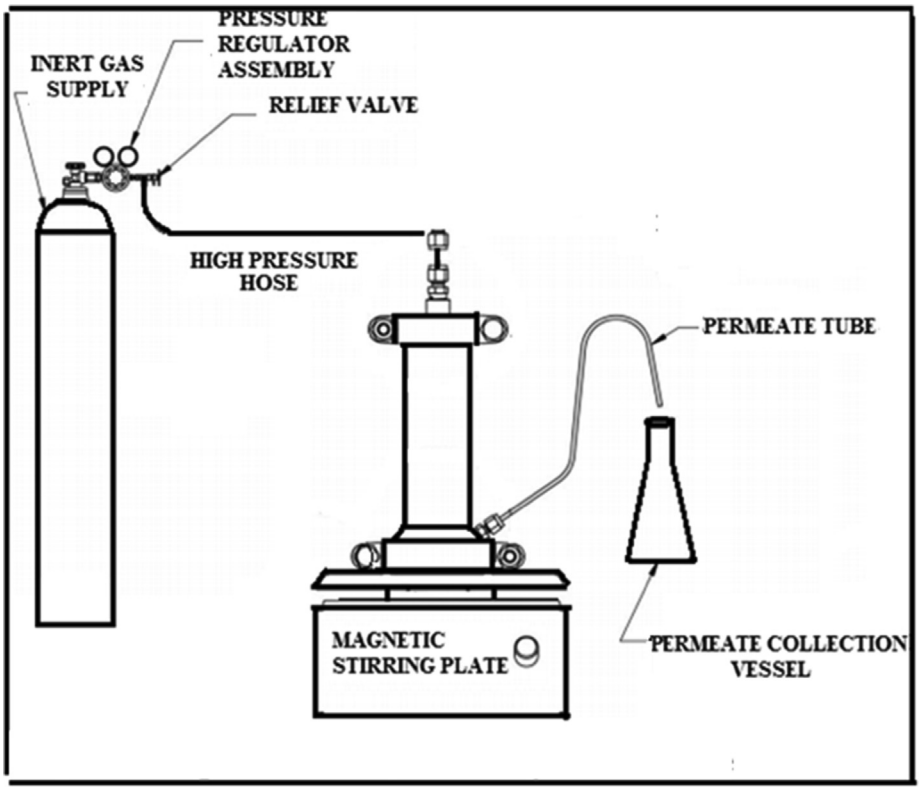

Fig. 2 Dead-end filtration system for RO membranes (Falath et al., 2016).

It has been reported that hydrophilic surfaces are less prone to biofouling (Fane and Fell, 1987; Hilal, 2005). Consequently, the synthesis of membranes with hydrophilic surfaces is favorable for fabricating biofouling resistant membranes. A thin layer of water is formed on top of hydrophilic surfaces. The significance of this layer is that it averts or reduces the absorption of foulants and it improves the permeability of the membrane (Kochkodan, 2012).

Fig. 3 demonstrates the effect of incorporating GO into the membrane matrix on hydrophilicity. The curve shows reduction in the water contact angle, which indicates that the conjugation of GO made the surface more hydrophilic. GO is hydrophilic in nature and contains carboxyl and hydroxyl groups amply on its basal planes and edges (Lee, 2013). Therefore, the presence of GO in membrane materials would induce hydrophilicity. Thus, the mixing of GO with the highly hydro-

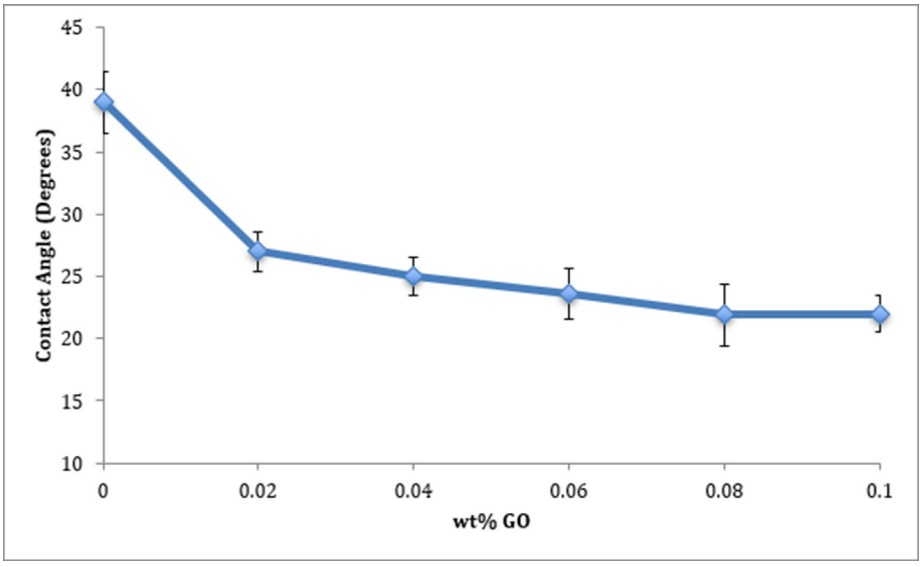

Fig. 3 Effect of infusing GO on the hydrophilicity of the surfaces.

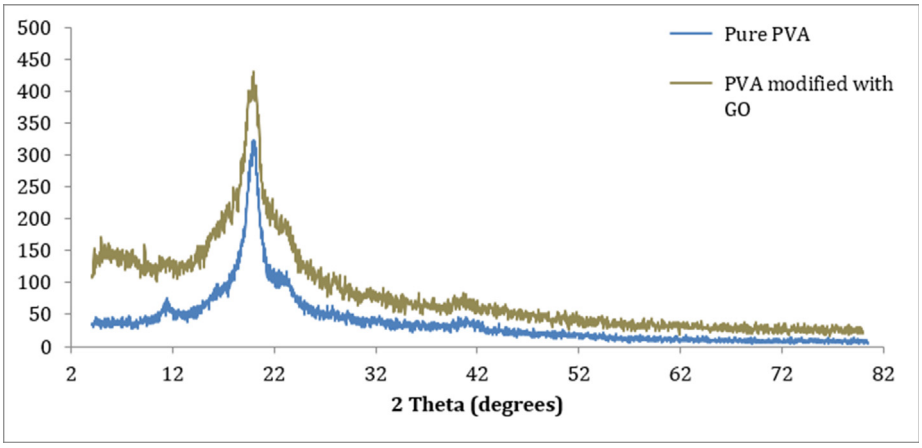

Fig. 4 XRD patterns of pure PVA and GO modified membranes.

philic PVA was expected to improve the overall hydrophilicity of the membrane surface (Li, 2019; Zhang, 2019).

3.2. X-Ray Diffraction.

X-ray diffraction characterizes the microstructure of the synthesized membranes. Diffraction peaks of the pure PVA and modified PVA membranes with 0.02 wt% GO are shown in Fig. 4. Peaks at 11.4°, 20.02°, 23.23°, and 40.89° are clearly visible for Pure PVA membrane. The strongest and the sharpest peak is at 20.02°. Those peaks are distinctive of Pure PVA and they clearly show the mostly crystalline behavior (Zhang, 2008). The modification of the membrane included additions of Pluronic F-127, GO and DGEBA. The strong peak at 20.02° became a little wider, which is due to crosslinking effect (Zhang, 2008). GO has a sharp peak at 10.88°, which corresponds to the (0 0 1) reflection. The absence of this peak in the XRD pattern indicates that there is good miscibility between GO and PVA (Stobinski, 2014; Sun, 2020).

3.3. Atomic force microscopy (AFM).

Surface roughness has a strong effect on biofouling inhibition (Elimelech, 1997). If the membrane surface becomes increasingly rougher, the surface area where microorganisms can adhere to will increase. Furthermore, the ridge-valley configuration, which is a trait of rough surfaces, enhances the buildup of foulants on the surface (Vrijenhoek et al., 2001). Fig. 5 shows the effect of GO inclusion on the surface roughness, measured by AFM. The figure shows that the surface roughness has declined considerably after modification with GO. That excellent effect on surface roughness is explained by the fact that conjugating GO with PVA causes an increase in casting solution's viscosity. This increase in viscosity impedes exchange rate of solvent/solute diffusion while dissolution casting process takes place, which leads to the formation of smooth membrane surfaces (Hegab and Zou, 2015; Khalid, 2015). The small increase in surface roughness with the inclusion of larger amounts of GO could be due to the fact that

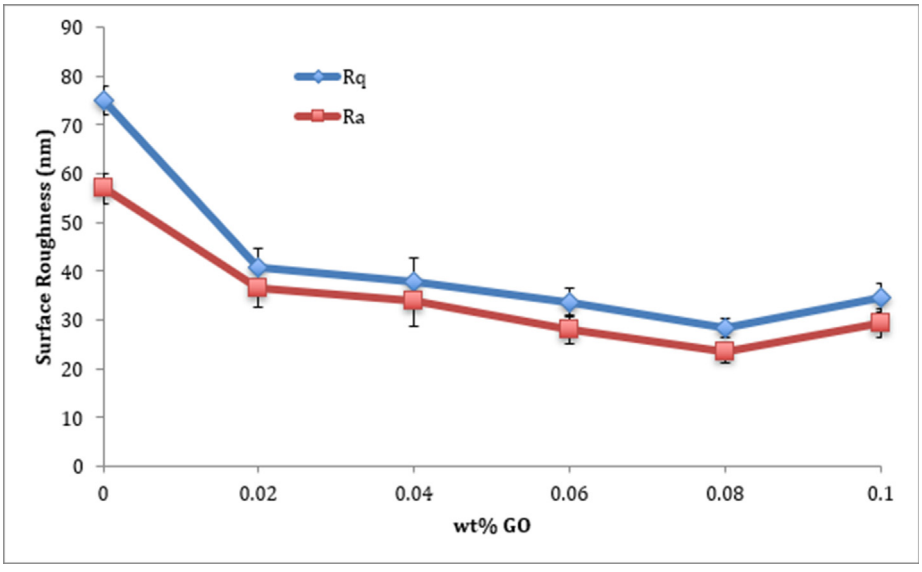

Fig. 5 Effect of GO loadings on surface roughness of PVA membranes.

excess amount of GO will adhere to the surface and form the unwanted ridge-valley structure that increase the surface roughness. That effect could be seen from surface morphology images taken by SEM, which will be discussed in the following section. Nevertheless, even with the abovementioned effect, the surface roughness has improved overall with the conjugation of GO. This result is excellent because, as mentioned earlier, reducing the surface roughness of the membrane leads to improved biofouling resistance and permeability.

3.4. Scanning electron microscope (SEM)

Reverse osmosis membranes are predominantly looked at as dense membranes since the pore size is ranging from 1 to 10 Å, which is basically the size of a free volume rather than a pore (Matin, 2011; Wijmans and Baker, 1995). Many researchers reported that Pluronic F-127 is a surfactant that helps in pore-forming (Loh, 2011; Susanto and Ulbricht, 2009). SEM images of Pure PVA and crosslinked PVA modified with Pluronic F-127 are shown in Fig. 6, (a) and (b), respectively. As anticipated, the incorporation of Pluronic F-127 resulted in relatively large pores that are clearly visible under SEM, ranging in size from 1 to 10 μm.

Fig. 6, (c-g), shows the SEM images of the membranes modified with GO. It is clear from the images that as the amount of GO increases, porosity and pore sizes decrease. Furthermore, excess amounts of GO are visible for the maximum loading of GO. An explanation to this behavior is that excess GO sheets inhabit the pores that have been formed by the incorporation of Pluronic F-127. When those pores are packed, excess amounts of GO will agglomerate and adhere to the membrane surface (Sun, 2020).

3.5. Mechanical properties

Graphene Oxide exhibits excellent mechanical properties (stiffness up to 40 GPa while remaining highly flexible and ductile). This is ascribed to the abundant hydrogen-bonding interac-

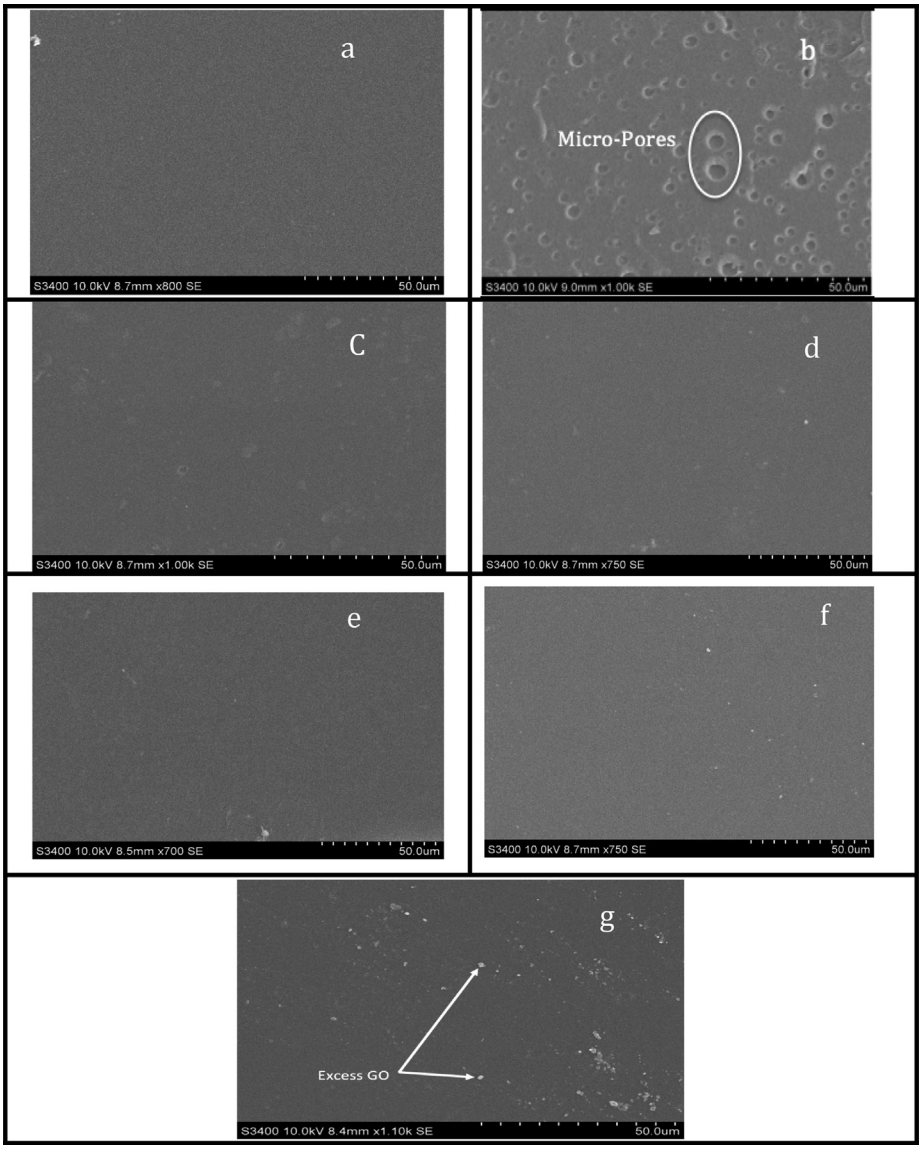

Fig. 6 SEM images of (a) pure PVA membrane, (b) PVA with Pluronic F-127 (c) PVA-G1, (d) PVA-G2, (e) PVA-G3, (f) PVA-G4 and (g) PVA-G5.

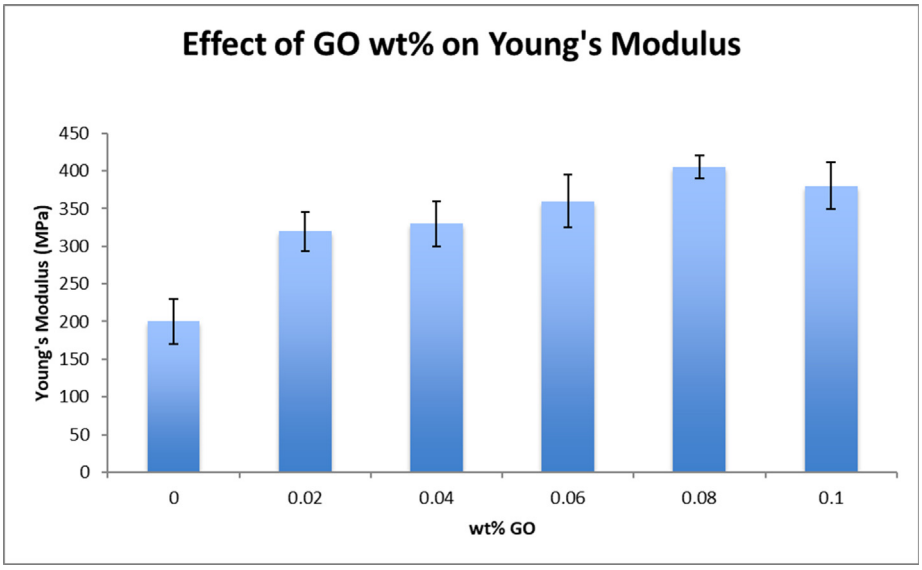

Fig. 7 Effect of GO inclusion on Young's modulus.

tions between neighboring sheets in the GO structure (Suk, 2010; Compton, 2012). Therefore, it is expected that the inclusion of GO within the matrix of crosslinked PVA will effectively enhance the overall mechanical stability of the membrane film.

Fig. 7 shows Young's modulus values for the newly synthesized membranes. The stiffness of the membranes, represented by Young's modulus, has improved significantly with the conjugation of GO. For PVA-G4, the stiffness of the membrane improved by more than 100%. The conjugation of GO into the PVA matrix acts like a physical crosslinking agent that forms denser network structure. That dense structure hinders internal structural relative movements during the tensile experiment, which enhances the stiffness of the membrane (Compton, 2012). These outcomes demonstrated the mechanical stability of the fabricated modified membranes. During practical conditions with extremely high reverse osmosis pressure of 800 Psi, the membranes functioned properly and withstood that high pressure without the need of a support or a substrate. Being able to utilize the membrane as is, without a substrate, negates the effect of internal concentration polarization which usually causes unnecessary increase in the applied pressure.

3.6. Effect of GO conjugation on separation effectiveness

Fig. 8 shows permeability and selectivity results, represented by permeate flux and salt rejection, for the membranes modified by GO. The permeability has increased considerably with the inclusion of GO. The maximum flux for PVA-G5 (92

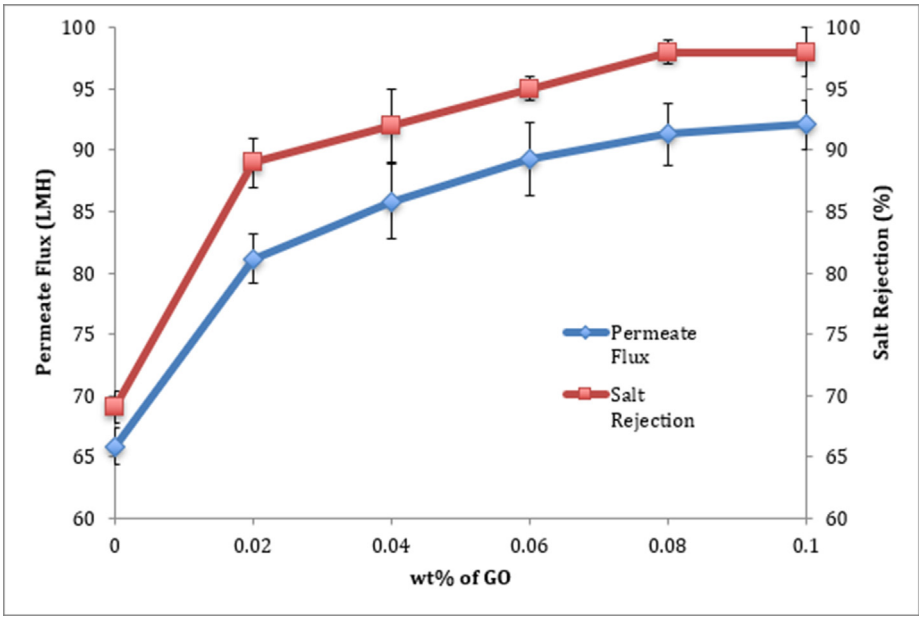

Fig. 8 Effect of GO wt% on flux and salt rejection.

LMH) is almost double the flux of commercially available RO membranes, which is an excellent achievement (Van Wagner, 2009). The obvious rationale is based on the enhancement of hydrophilicity. It has been reported by many researchers that improving the hydrophilicity of the surface generally enhances the water flux through the membrane (Fane and Fell, 1987; Hilal, 2005).

The figure also shows the effect of inclusion of GO on selectivity. It is very evident that conjugating slight amounts of GO into the polymer matrix improved the salt rejection immensely. Selectivity improved from around 70% to around 98% for PVA-G4 and PVA-G5. The inclusion of GO into PVA membranes resulted in a semi-network structure that obstructed the stream of salt molecules (Mahmoud, 2015). It is noteworthy that the enhancement occurred in both permeability and selectivity. The usual trend is that it is a compromise between the two properties. The unique characteristics of GO, mainly its high hydrophilicity and its physical crosslinking ability, made it possible to gain both at the same time.

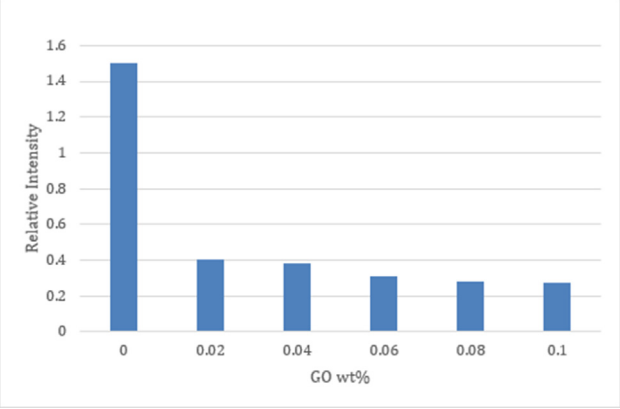

Fig. 9 Relative amounts of bacterial cells adhering onto membrane surfaces.

3.7. Effect of GO conjugation on biofouling resistance

The antibacterial property of the membrane was analyzed utilizing JIS L 1902–2002 methodology while using Escherichia coli (E. coli) as model bacteria. It was observed that conical flasks with unmodified membranes looked contaminated, which indicates the bacterial growth, whereas the other flasks with GO modification displayed almost a clear solution. Fig. 9 shows the optical densities (OD) of the membranes. The high OD of the pristine membranes indicates the induction of E. coli on the membrane surfaces. Contrariwise, OD of the GO modified membranes indicated that there was an insignificant bacterial growth. Therefore, this test clearly showed the effect of GO inclusion on anti-bacterial property of the membrane. The reduction of the optical density was around 130%, which is a vast improvement of the antibacterial property that leads to biofouling resistance eventually. The enhancement of the antimicrobial activity of the membrane is due to the improved hydrophilicity of the membranes as has been shown earlier. Due to hydrophobic-hydrophobic interactions, bacteria, which are mostly hydrophobic, tend to adhere to hydrophobic surfaces. Furthermore, as the surface roughness reduces, bacteria find it more difficult to attach to the surface (Padil, 2015). Besides, some researchers proved that GO defective edges provide active sites to produce reactive oxygen species that cause residual stresses. Theses stresses can cause damage to bacterial cells (Li, 2019).

3.8. Effect of GO inclusion on Membrane's chlorine resistance

Fig. 10 shows selectivity of the membranes before and after Chlorination. It is clear that the unmodified membrane has low Chlorine tolerance as the selectivity dramatically declined from 69% to 41%, a 40% decrease in salt rejection percentage. Conversely, once GO was conjugated, the decline in salt rejection became negligible, which implies that the conjugation with GO made the membrane chemically stable and more tolerable to harsh environments.

Commercially available RO membranes fabricated using Polyamide (PA) are known to be severely susceptible to Chlo-

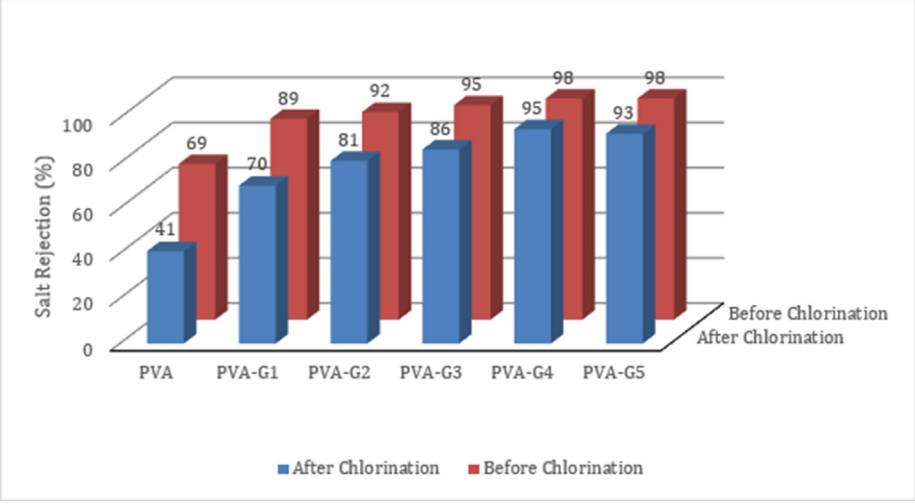

Fig. 10 Effect of GO wt% on the Chlorine tolerance of the membrane.

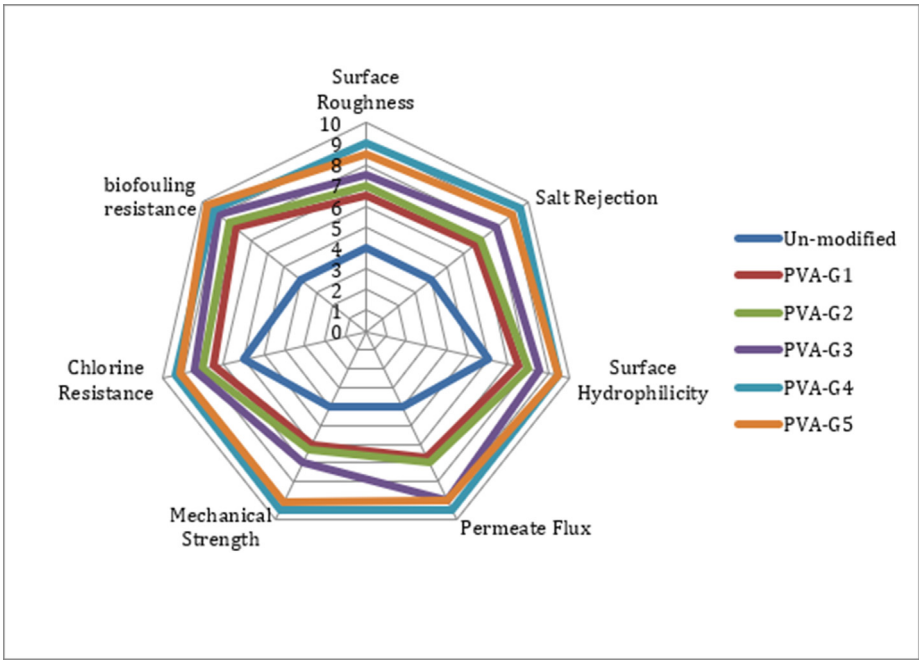

Fig. 11 Target plot for overall performance comparison between pristine PVA and modified membranes.

rine attack even if lower concentrations of Chlorine are used compared to the concentrations used in this research. As an example, SW30HR, Dow FilmTec, a commercially available RO membrane, showed almost 25% reduction in selectivity in less Chlorine concentrations (Knoell, 2006; Park, 2008). The membranes fabricated in this study possess superior Chlorine resistance compared to commercially available membranes. This outcome is essential as it reduces the need for de-Chlorination pretreatment which is used often commercially to protect the membrane's surface (Zhang, 2014).

Fig. 11 shows a target plot where membranes with various concentrations of GO are ranked according to their performance excellence. Inner loops represent poor performance while outer loops represent flawlessness. It is clearly shown that the conjugation of GO had a tremendous positive enhancement of overall performance compared to pristine PVA membrane. Membranes PVA-G4 and PVA-G5 provided optimal overall properties.

4. Conclusion

The present study was designed to determine the effect of conjugating GO nanosheets with crosslinked PVA membranes on the efficiency of the RO membranes. The novelty of this research is that the membranes are utilized as stand-alone without any substrate. As mentioned earlier, achieving improved results without a substrate is an excellent outcome of this research. The results of this investigation and previous investigations of the author and his collaborators showed that the fabricated PVA RO membranes overcame common issues with PVA like swelling effect and membrane rupture under high pressure. This was achieved by crosslinking and proper selection of modifiers.

Conjugating crosslinked PVA with GO improved the performance of the membranes in general. That includes enhancement of hydrophilicity, reduction of surface roughness and improvement in selectivity, biofouling resistance and mechanical and chemical stability. This study paves the way for the utilization of PVA as an active layer in RO plants. Further study is needed to test the membranes in crossflow setup which better mimics the commercial RO setup.

Declaration of Competing Interest

The author declares that there is no conflict of interest.

Acknowledgement

The author would like to acknowledge the Deanship of Research, King Fahd University of Petroleum and Minerals for its financial support through project# SR161002.

References

Amanda, A. et al, 2000. Semicrystalline poly(vinyl alcohol) ultrafiltration membranes for bioseparations. J. Membr. Sci. 176 (1), 87–95.

Anis, S.F., Lalia, B.S., Hashaikeh, R., 2014. Controlling swelling behavior of poly (vinyl) alcohol via networked cellulose and its application as a reverse osmosis membrane. Desalination 336, 138–145.

Augustine, M.S. et al, 2012. Excellent UV absorption in spin-coated thin films of oleic acid modified zinc oxide nanorods embedded in polyvinyl alcohol. J. Phys. Chem. Solids 73 (3), 396–401.

Baker, J.S., Dudley, L.Y., 1998. Biofouling in membrane systems – a review. Desalination 118 (1–3), 81–89.

Bano, S. et al, 2014. Chlorine resistant binary complexed NaAlg/PVA composite membrane for nanofiltration. Sep. Purif. Technol. 137, 21–27.

Barona, G.N.B., Choi, M., Jung, B., 2012. High permeate flux of PVA/PSf thin film composite nanofiltration membrane with aluminosil-

icate single-walled nanotubes. J. Colloid Interface Sci. 386, 189–197.
Bezuidenhout, D. et al, 1998. Reverse osmosis membranes prepared from potassium peroxydisulphate-modified poly(vinyl alcohol). Desalination 116 (1), 35–43.
Bolto, B. et al, 2009. Crosslinked poly(vinyl alcohol) membranes. Prog. Polym. Sci. 34 (9), 969–981.
Cha, W.-I., Hyon, S.-H., Ikada, Y., 1993. Microstructure of poly(vinyl alcohol) hydrogels investigated with differential scanning calorimetry. Die Makromolekulare Chemie 194 (9), 2433–2441.
Choi, W. et al, 2013. Layer-by-layer assembly of graphene oxide nanosheets on polyamide membranes for durable reverse-osmosis applications. ACS Appl. Mater. Interfaces 5 (23), 12510–12519.
Cohen-Tanugi, D., Grossman, J.C., 2015. Nanoporous graphene as a reverse osmosis membrane: recent insights from theory and simulation. Desalination 366, 59–70.
Compton, O.C., et al., 2012. Tuning the mechanical properties of graphene oxide paper and its associated polymer nanocomposites by controlling cooperative intersheet hydrogen bonding 6(3), 2008–2019.
De Beer, D., Stoodley, P., 2006. Microbial Biofilms. Prokaryotes: A Handbook on the Biology of Bacteria, Vol 1, Third Edition: Symbiotic Associations, Biotechnology, Applied Microbiology, ed. M. Dworkin, et al. 2006, New York: Springer. 904-937.
Elimelech, M. et al, 1997. Role of membrane surface morphology in colloidal fouling of cellulose acetate and composite aromatic polyamide reverse osmosis membranes. J. Membr. Sci. 127 (1), 101–109.
Falath, W., Sabir, A., Jacob, K.I., 2016. Highly improved reverse osmosis performance of novel PVA/DGEBA cross-linked membranes by incorporation of Pluronic F-127 and MWCNTs for water desalination. Desalination 397, 53–66.
Falath, W., Sabir, A., Jacob, K.I., 2017. Novel reverse osmosis membranes composed of modified PVA/Gum Arabic conjugates: Biofouling mitigation and chlorine resistance enhancement. Carbohydr. Polym. 155, 28–39.
Fane, A.G., Fell, C.J.D., 1987. A review of fouling and fouling control in ultrafiltration. Desalination 62, 117–136.
Fang, T.-H., Chang, W.-J., 2003. Effects of AFM-based nanomachining process on aluminum surface. J. Phys. Chem. Solids 64 (6), 913–918.
Flemming, H.C., 2002. Biofouling in water systems – cases, causes and countermeasures. Appl. Microbiol. Biotechnol. 59 (6), 629–640.
Flynn, E.J. et al, 2013. Pervaporation performance enhancement through the incorporation of mesoporous silica spheres into PVA membranes. Sep. Purif. Technol. 118, 73–80.
Gebben, B. et al, 1985. Intramolecular crosslinking of poly(vinyl alcohol). Polymer 26 (11), 1737–1740.
Giménez, V., Mantecón, A., Cádiz, V., 1996. Crosslinking of poly (vinyl alcohol) using dianhydrides as hardeners. J. Appl. Polym. Sci. 59 (3), 425–431.
Guo, R. et al, 2007. Novel PVA–silica nanocomposite membrane for pervaporative dehydration of ethylene glycol aqueous solution. Polymer 48 (10), 2939–2945.
Hegab, H.M., Zou, L., 2015. Graphene oxide-assisted membranes: fabrication and potential applications in desalination and water purification. J. Membr. Sci. 484, 95–106.
Herzberg, M., Elimelech, M., 2007. Biofouling of reverse osmosis membranes: role of biofilm-enhanced osmotic pressure. J. Membr. Sci. 295 (1–2), 11–20.
Hilal, N. et al, 2005. Methods employed for control of fouling in MF and UF membranes: a comprehensive review. Sep. Sci. Technol. 40 (10), 1957–2005.
Hu, S.Y. et al, 2012. Composite membranes comprising of polyvinylamine-poly(vinyl alcohol) incorporated with carbon nanotubes for dehydration of ethylene glycol by pervaporation. J. Membr. Sci. 417–418, 34–44.
Hu, M., Mi, B.X., 2013. Enabling graphene oxide nanosheets as water separation membranes. Environ. Sci. Technol. 47 (8), 3715–3723.
Huang, H.-H. et al, 2019. Fabrication of reduced graphene oxide membranes for water desalination. J. Membr. Sci. 572, 12–19.
Huang, R.Y.M., Rhim, J.W., 1993. Modification of poly(vinyl alcohol) using maleic acid and its application to the separation of acetic acid-water mixtures by the pervaporation technique. Polym. Int. 30 (1), 129–135.
Ishihara, K., Hanyuda, H., Nakabayashi, N., 1995. Synthesis of phospholipid polymers having a urethane bond in the side chain as coating material on segmented polyurethane and their platelet adhesion-resistant properties. Biomaterials 16 (11), 873–879.
Iwasaki, Y., Yamasaki, A., Ishihara, K., 2003. Platelet compatible blood filtration fabrics using a phosphorylcholine polymer having high surface mobility. Biomaterials 24 (20), 3599–3604.
Johnson, D.J., Hilal, N., 2021. Can graphene and graphene oxide materials revolutionise desalination processes?. Desalination 500, 114852.
Kang, D.-Y. et al, 2012. Single-walled aluminosilicate nanotube/poly (vinyl alcohol) nanocomposite membranes. ACS Appl. Mater. Interfaces 4 (2), 965–976.
Khalid, A. et al, 2015. Preparation and properties of nanocomposite polysulfone/multi-walled carbon nanotubes membranes for desalination. Desalination 367, 134–144.
Kim, S.G. et al, 2013. Novel thin nanocomposite RO membranes for chlorine resistance. Desalin. Water Treat. 51 (31–33), 6338–6345.
Kim, H.K., Chung, H.J., Park, T.G., 2006. Biodegradable polymeric microspheres with "open/closed" pores for sustained release of human growth hormone. J. Control. Release 112 (2), 167–174.
Knoell, T., 2006. Chlorine's impact on the performance and properties of polyamide membranes. Ultrapure Water 23 (3), 24–31.
Kochkodan, V., Hilal, N., 2015. A comprehensive review on surface modified polymer membranes for biofouling mitigation. Desalination 356, 187–207.
Kochkodan, V., 2012. Reduction of Membrane Fouling by Polymer Surface Modification, in Membrane Modification: Technology and Applications, N. Hilal, Khayet, M. and Wright, C. J., Editor. 2012, CRC Press, ProQuest ebrary: London, GBR. p. 41–76.
Korsmeyer, R.W., Peppas, N.A., 1981. Effect of the morphology of hydrophilic polymeric matrices on the diffusion and release of water soluble drugs. J. Membr. Sci. 9 (3), 211–227.
Kwok, D.Y., Neumann, A.W., 1999. Contact angle measurement and contact angle interpretation. Adv. Colloid Interface Sci. 81 (3), 167–249.
Le, V.T. et al, 2021. Graphene-based nanomaterial for desalination of water: a systematic review and meta-analysis. Food Chem. Toxicol. 148, 111964.
Lee, K.P., Arnot, T.C., Mattia, D., 2011. A review of reverse osmosis membrane materials for desalination-development to date and future potential. J. Membr. Sci. 370 (1–2), 1–22.
Lee, J., et al., Graphene oxide nanoplatelets composite membrane with hydrophilic and antifouling properties for wastewater treatment. 448, p. 223–230.
Li, N. et al, 2010. Preparation and properties of PVDF/PVA hollow fiber membranes. Desalination 250 (2), 530–537.
Li, X. et al, 2014. Desalination of dye solution utilizing PVA/INDF hollow fiber composite membrane modified with TiO2 nanoparticles. J. Membr. Sci. 471, 118–129.
Li, Y. et al, 2019. Comparison of performance and biofouling resistance of thin- film composite forward osmosis membranes with substrate/ active layer modified by graphene oxide. RSC Adv. 9 (12), 6502–6509.
Li, D., Yan, Y., Wang, H., 2016. Recent advances in polymer and polymer composite membranes for reverse and forward osmosis processes. Prog. Polym. Sci. 61, 104–155.
Liu, M. et al, 2011. Thin-film composite polyamide reverse osmosis membranes with improved acid stability and chlorine resistance by

coating N-isopropylacrylamide-co-acrylamide copolymers. Desalination 270 (1–3), 248–257.
Liu, Y. et al, 2013. High-flux microfiltration filters based on electrospun polyvinylalcohol nanofibrous membranes. Polymer 54 (2), 548–556.
Liu, M. et al, 2014. Enhancing the permselectivity of thin-film composite poly(vinyl alcohol) (PVA) nanofiltration membrane by incorporating poly(sodium-p-styrene-sulfonate) (PSSNa). J. Membr. Sci. 463, 173–182.
Liu, M. et al, 2015. Improving fouling resistance and chlorine stability of aromatic polyamide thin-film composite RO membrane by surface grafting of polyvinyl alcohol (PVA). Desalination 367, 11–20.
Loh, C.H. et al, 2011. Fabrication of high performance polyethersulfone UF hollow fiber membranes using amphiphilic Pluronic block copolymers as pore-forming additives. J. Membr. Sci. 380 (1–2), 114–123.
Lv, C.L. et al, 2007. Enhanced permeation performance of cellulose acetate ultrafiltration membrane by incorporation of Pluronic F127. J. Membr. Sci. 294 (1–2), 68–74.
Macho, V. et al, 1994. Modified poly(vinyl alcohol) as a dispersant in suspension polymerization of vinyl chloride: 3. Acetalized poly (vinyl alcohol). Polymer 35 (26), 5773–5777.
Mahmoud, K.A. et al, 2015. Functional graphene nanosheets: the next generation membranes for water desalination. Desalination 356, 208–225.
Malaeb, L., Ayoub, G.M., 2011. Reverse osmosis technology for water treatment: state of the art review. Desalination 267 (1), 1–8.
Matin, A. et al, 2011. Biofouling in reverse osmosis membranes for seawater desalination: phenomena and prevention. Desalination 281, 1–16.
Misdan, N., Lau, W.J., Ismail, A.F., 2012. Seawater reverse Osmosis (SWRO) desalination by thin-film composite membrane-current development, challenges and future prospects. Desalination 287, 228–237.
Oki, T., Kanae, S., 2006. Global hydrological cycles and world water resources. Science 313 (5790), 1068–1072.
Padil, V.V.T. et al, 2015. Synthesis, fabrication and antibacterial properties of a plasma modified electrospun membrane consisting of gum Kondagogu, dodecenyl succinic anhydride and poly (vinyl alcohol). Surf. Coat. Technol. 271, 32–38.
Park, H.B. et al, 2008. Highly chlorine-tolerant polymers for desalination. Angew. Chem. Int. Ed. 47 (32), 6019–6024.
Petersen, R.J., 1993. Composite reverse osmosis and nanofiltration membranes. J. Membr. Sci. 83 (1), 81–150.
Pourjafar, S., Rahimpour, A., Jahanshahi, M., 2012. Synthesis and characterization of PVA/PES thin film composite nanofiltration membrane modified with TiO2 nanoparticles for better performance and surface properties. J. Ind. Eng. Chem. 18 (4), 1398–1405.
Presumido, P.H. et al, 2020. Large area continuous multilayer graphene membrane for water desalination. Chem. Eng. J. 127510
Rajaeian, B. et al, 2015. Improved separation and antifouling performance of PVA thin film nanocomposite membranes incorporated with carboxylated TiO2 nanoparticles. J. Membr. Sci. 485, 48–59.
Ridgway, H.F., 1988. Microbial Adhesion and Biofouling of Reverse Osmosis Membranes. In: Parekh, B.S. (Ed.), Reverse Osmosis Technology: Applications for High-Purity Water Production. Marcel Dekker, New York, Basel, pp. 429–481.
Ridgway, H.F.a.S., J, Biofouling of Reverse Osmosis Membranes, in Biofouling and Biocorrosion in Industrial Water Systems, H.C.a.G. Flemming, G. G., Editor. 1990, Springer-Verlag. p. 81–111.
Sadr Ghayeni, S.B. et al, 1998. Adhesion of waste water bacteria to reverse osmosis membranes. J. Membr. Sci. 138 (1), 29–42.
Shang, Y., Peng, Y., 2007. Research of a PVA composite ultrafiltration membrane used in oil-in-water. Desalination 204 (1–3), 322–327.
Shang, Y., Peng, Y., 2008. UF membrane of PVA modified with TDI. Desalination 221 (1–3), 324–330.
Shannon, M.A. et al, 2008. Science and technology for water purification in the coming decades. Nature 452 (7185), 301–310.
Stobinski, L. et al, 2014. Graphene oxide and reduced graphene oxide studied by the XRD, TEM and electron spectroscopy methods. J. Electron Spectrosc. Relat. Phenom. 195, 145–154.
Subramani, A., Jacangelo, J.G., 2015. Emerging desalination technologies for water treatment: a critical review. Water Res. 75, 164–187.
Suk, J.W., et al., 2010. Mechanical properties of monolayer graphene oxide. 2010. 4(11): p. 6557-6564.
Sun, J. et al, 2020. Tailoring the microstructure of poly(vinyl alcohol)-intercalated graphene oxide membranes for enhanced desalination performance of high-salinity water by pervaporation. J. Membr. Sci. 599, 117838.
Susanto, H., Ulbricht, M., 2009. Characteristics, performance and stability of polyethersulfone ultrafiltration membranes prepared by phase separation method using different macromolecular additives. J. Membr. Sci. 327 (1–2), 125–135.
Van Wagner, E.M. et al, 2009. Effect of crossflow testing conditions, including feed pH and continuous feed filtration, on commercial reverse osmosis membrane performance. J. Membr. Sci. 345 (1–2), 97–109.
Vrijenhoek, E.M., Hong, S., Elimelech, M., 2001. Influence of membrane surface properties on initial rate of colloidal fouling of reverse osmosis and nanofiltration membranes. J. Membr. Sci. 188 (1), 115–128.
Wijmans, J.G., Baker, R.W., 1995. The solution-diffusion model: a review. J. Membr. Sci. 107 (1–2), 1–21.
Yajima, S. et al, 2002. Ion-sensor property and blood compatibility of neutral-carrier-type poly(vinyl chloride) membranes coated by phosphorylcholine polymers. Anal. Chim. Acta 463 (1), 31–37.
Yang, Y. et al, 2021. Microstructure evolution and texture tailoring of reduced graphene oxide reinforced Zn scaffold. Bioact. Mater. 6 (5), 1230–1241.
Yee, K.F. et al, 2014. Novel MWCNT-buckypaper/polyvinyl alcohol asymmetric membrane for dehydration of etherification reaction mixture: Fabrication, characterisation and application. J. Membr. Sci. 453, 546–555.
You, H. et al, 2012. Low pressure high flux thin film nanofibrous composite membranes prepared by electrospraying technique combined with solution treatment. J. Membr. Sci. 394–395, 241–247.
Zhang, L.-Z. et al, 2008. Synthesis and characterization of a PVA/LiCl blend membrane for air dehumidification. J. Membr. Sci. 308 (1–2), 198–206.
Zhang, Y. et al, 2014. Highly chlorine-resistant multilayer reverse osmosis membranes based on sulfonated poly(arylene ether sulfone) and poly(vinyl alcohol). Desalination 336, 58–63.
Zhang, M. et al, 2019. Effect of substrate on formation and nanofiltration performance of graphene oxide membranes. J. Membr. Sci. 574, 196–204.